Karlsruher Institut für Technologie

Crack-tip models by Irwin and Dugdale for hydroxyl-damaged crack-tip zones

T. Fett, K.G. Schell, C. Bucharsky

KIT SCIENTIFIC WORKING PAPERS 173

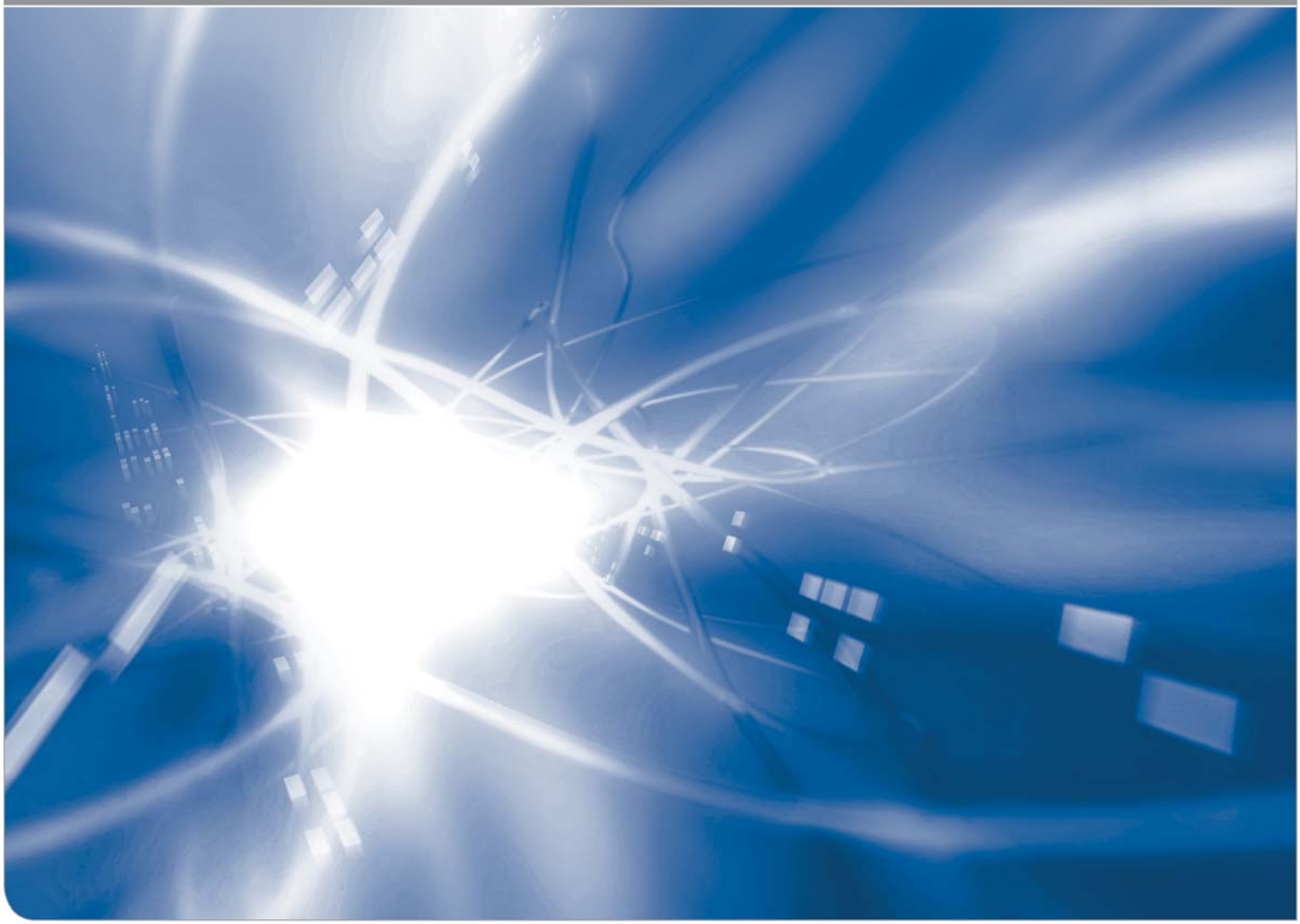

KIT – Universität des Landes Baden-Württemberg und nationales Forschungszentrum in der Helmholtz-Gemeinschaft

IAM Institute for Applied Materials

Impressum

Karlsruher Institut für Technologie (KIT)
www.kit.edu

2021

ISSN: 2194-1629

Abstract

Due to the hydroxyl generation, the silica network ahead of crack tips is damaged. The consequence is a damaged crack-tip zone showing a reduced Young's modulus. The linear-elastic fracture mechanical treatment by application of stress intensity factors becomes doubtful especially for large zones. In this report, we use a description via well-known models of Elastic-Plastic Fracture Mechanics, namely, the models by Irwin and Dugdale.

As an application we compared the results with experimental observations on crack profiles from literature. The computed and observed Crack-Tip Opening Displacements (CTOD) were found to be in good agreement.

Contents

1. Introduction

The reaction of water and silica in the surface diffusion zone affects the fracture mechanics stress intensity factor K at the tips of cracks. At temperatures $T < 450°C$, the equilibrium constant k_1 of the water/silica-reaction

$$\equiv\text{Si-O-Si}\equiv + H_2O \leftrightarrow \equiv\text{SiOH+HOSi}\equiv \tag{1}$$

is given by

$$k_1 = \frac{S}{C}. \tag{2}$$

where, $S = [\equiv\text{SiOH}]$, is the concentration of the hydroxyl groups in the silica network and $C = [H_2O]$ the concentration of unreacted water.

According to Le Chatelier [1], the equation governing the equilibrium constant is

$$\frac{\partial \ln k_1}{\partial p} = -\frac{\Delta\overline{V}}{RT}. \tag{3}$$

where p is pressure, $\Delta\overline{V}$ is the reaction volume, R the universal gas constant, and T the temperature in °K.

In gases and liquids, the loading is always hydrostatic. In a solid the situation is more complicated, since the individual stress components σ_x, σ_y, σ_z are in general independent of each other and are not necessarily hydrostatic. Especially in uniaxial tension or compression, the hydrostatic stress deviates clearly from the tensile stress. In contrast to this, the stress state ahead of crack tips is more hydrostatic since the stress in the prospective plane and the stress normal on this plane are identical, $\sigma_x=\sigma_y$, and the stress σ_z is very close to the tip: $\sigma_z=\nu(\sigma_x+\sigma_y)$, ν=Poisson's ratio.

By replacing the hydrostatic pressure p by the hydrostatic stress σ_h in a solid

$$\sigma_h = \tfrac{1}{3}(\sigma_x + \sigma_y + \sigma_z) \tag{4}$$

we obtain with the hydroxyl concentration S_0 for $\sigma_h=0$

$$S = S_0 \exp\left(\frac{\sigma_h \Delta\overline{V}}{RT}\right) \quad , \quad \sigma_h = -p \tag{5}$$

The singular hydrostatic near-tip stresses together with eq.(5) implies that in the high crack-tip stress field nearly all water is present exclusively in form of hydroxyl S.

2. Motivation for the application of the plasticity models

Subcritical crack growth tests in heavy water were carried out on DCDC specimens of silica by Lechenault et al. [2]. The water entrance into the fracture surfaces, formed by the passage of the crack exposed to deuterium oxide D_2O, was evaluated with a

neutron reflection technique to measure the penetration of the deuterium oxide into the silica glass. The authors found a satisfactory fit to the reflection data by assuming that the water concentration was constant at the surface up to a distance of L, followed by an exponential decrease in concentration for distances greater than L.

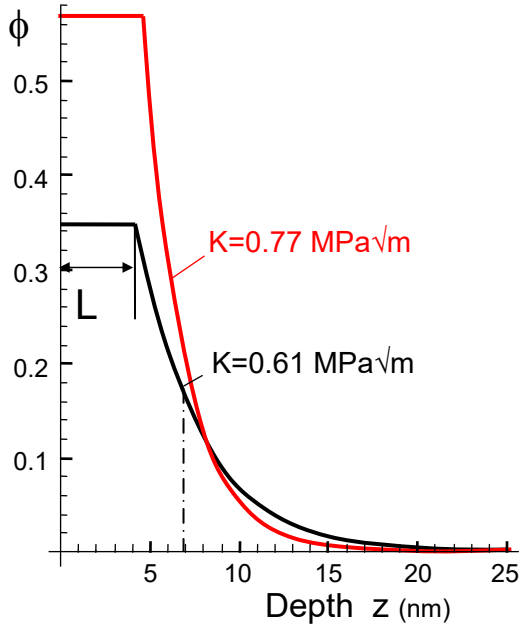

Fig. 1 Water profiles expressed by the neutron reflectivity ϕ measured by Lechenault et al. [2] on DCDC specimens fractured in heavy water.

Lechenault et al. [2] fitted their results by the expression

$$C_w / C_w(0) = \begin{cases} 1 & \text{for} \quad z \le L \\ \exp[-(z-L)/\eta] & \text{for} \quad z > L \end{cases} \tag{6}$$

and found the parameters L=4.3 nm, η=3.5 nm for a region of low crack rates ($v \approx 10^{-8}$ m/s) at K= 0.61 MPa·m$^{1/2}$ and L=4.6 nm, η=2.3 nm for higher crack rates ($v \approx 4\ 10^{-6}$ m/s) at K= 0.77 MPa·m$^{1/2}$. These water profiles are illustrated in Fig. 1. Their flat behaviour over an extended region calls for the application of the Dugdale- and the Irwin-model developed for linear-elastic perfectly plastic materials.

3 Hydroxyl damage and Young's modulus

The hydroxyl generation by the reaction eq.(1) causes damage since the originally intact silica ring structure is cracked by the water attack. One of the consequences of such damage is the reduction of Young's modulus E. In order to describe this E-decrease, we used in [3] the rather simple damage model proposed by Phani and

Niyogi [4]. When E_D is the modulus in the damaged state and E_0 the value for undamaged silica, we could derive the relation [3]

$$\frac{E_D}{E_0} = (1-\gamma S)^2 = (1 - S/S_{\max})^2 \tag{7}$$

with γ=5.3 [4.35, 6.25] (90%-CI in brackets). The hydroxyl concentration at which the Young's modulus disappears is $S_{\max}$ =1/γ= 0.188 [0.16, 0.23]. Under the condition that the damage is isotropic and Poisson's ratio ν remains sufficiently constant [5], the multiaxiality in damaged states remains unchanged.

When the reaction (1) has taken place, the applied stresses $\sigma_{h,appl}$ decrease according to eq.(5) to σ_h and the hydroxyl concentration is

$$S = S_0 \exp[\mu \sigma_h], \qquad \mu = \frac{\Delta \overline{V}}{RT} \tag{8}$$

Consequently, the hydroxyl concentration as a function of the hydrostatic stress, eq.(5), can be written in terms of the applied ones as

$$S = S_0 \exp[\mu \sigma_{h,appl} (1 - S/S_{\max})^2] \tag{9}$$

Equation (9) is an implicit equation since the unknown concentration *S* occurs on both sides. The solution can be found by numerical methods (e.g. by the subroutine *FindRoot* of Mathematica [6]).

Figure 2a shows the hydroxyl concentration as a function of $\sigma_{h,appl}$ and S_0. Figure 2b represents the hydrostatic stress under damage conditions as a function of the externally applied hydrostatic stress for several initial hydroxyl concentrations S_0. The maximum hydrostatic stress, asymptotically reached for $\sigma_{h.appl} \to \infty$, is according to eq.(5)

$$\sigma_{h,D,\max} = -\frac{1}{\mu} \mathrm{Log}\left[\frac{S_0}{S_{\max}}\right] \tag{10}$$

The true stresses $\sigma_{h,D}$ of Fig. 2b may be simplified by a bi-linear description as introduced by the dash-dotted lines in Fig. 2b. In this case, the maximum possible stress in the damaged state is depending on the parameter μ, containing the temperature. In the sense of an upper limit solution, the stresses can be approximated as

$$\sigma_{h,D} = \begin{cases} \sigma_{h,appl} & \text{for} \quad \sigma_{h,appl} < \sigma_{h,D,\max} \\ \sigma_{h,D,\max} & \text{else} \end{cases} \tag{11}$$

It is clear that use of the approximation of the curves in Fig. 2b by eq.(11) must overestimate the real stresses.

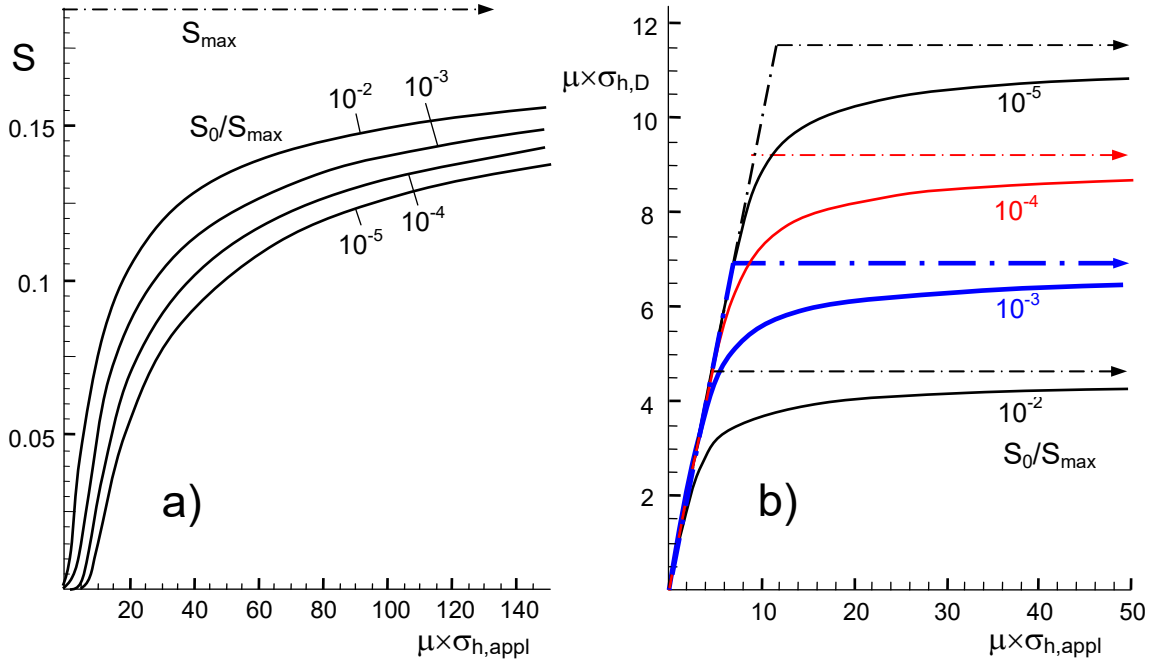

Fig. 2 a) Hydroxyl concentration vs. applied stress under condition of constant strains, b) hydrostatic stress in the damaged material $\sigma_{h,D}$ as a function of the applied hydrostatic stress $\sigma_{h,appl}$ and the initial hydroxyl concentration S_0 with the abbreviation μ defined by eq.(8), limits of hydrostatic stress and approximation by an upper bound description (dash-dotted straight lines).

4 Irwin and Dugdale model

Due to the damage via hydroxyl generation, the stress-strain behavior at a crack tip is no longer linear. By application of the bi-linearized dependency, eq.(11), fracture mechanics problems can be approximately solved applying the well-known Irwin and Dugdale models, originally developed for elastic/plastic material behaviour.

Whereas the Irwin model [7] is preferred for circular "plastic zones", the Dugdale model [8] describes also plastic deformations in a narrow strip in front of the crack.

According to these models the "length" L of the "plastic" zone, (Fig. 3a), is under plane stress conditions

$$L_{Irwin} = \frac{1}{\pi}\left(\frac{K_{appl}}{\sigma_Y}\right)^2, \quad L_{Dugdale} = \frac{\pi}{8}\left(\frac{K_{appl}}{\sigma_Y}\right)^2 \tag{12}$$

where σ_Y is the "yield stress" for the case of a linear-elastic/ideal-plastic material. Whereas in the Irwin model the size of the "plastic zone" was computed from "yield"-condition $\sigma_{appl,y}=\sigma_Y$ and along the prospective crack plane by force equilibrium, the size of the Dugdale zone results from the condition that the stress intensity factor for the fictive crack in Fig. 3a disappears. So the shape of the zones is not fixed, especially not for the Dugdale zone. The latter is mostly concentrated along the x-axis.

In the Dugdale model the stresses are normal to the crack plane, $\sigma=\sigma_y$. In this case, the ratio of the hydrostatic stress to the normal stress is

$$\sigma_h / \sigma_y = \tfrac{1}{3} \tag{13}$$

The opening at the tip of the physical crack, called *Crack Tip Opening Displacement* (CTOD), δ_t, is illustrated in Fig. 3b and determined in Fig. 4b

$$\delta_{t,Irwin} = \frac{4}{\pi}\frac{K_{appl}^2}{E\sigma_Y},\ \delta_{t,Dugdale} = \frac{K_{appl}^2}{E\sigma_Y} \tag{14}$$

For the damage zone ahead a crack, the Irwin model may be preferred here. The normal stress along the prospective crack plane is according to (13):

$$\sigma_Y = 3\sigma_{h,D.\max} \tag{15}$$

In the derivation of the Dugdale formula, it was assumed that there exists an internal through-the-thickness crack in an infinite plate and that the yield stress is constant over the zone size *L* regardless of the locally varying strains.

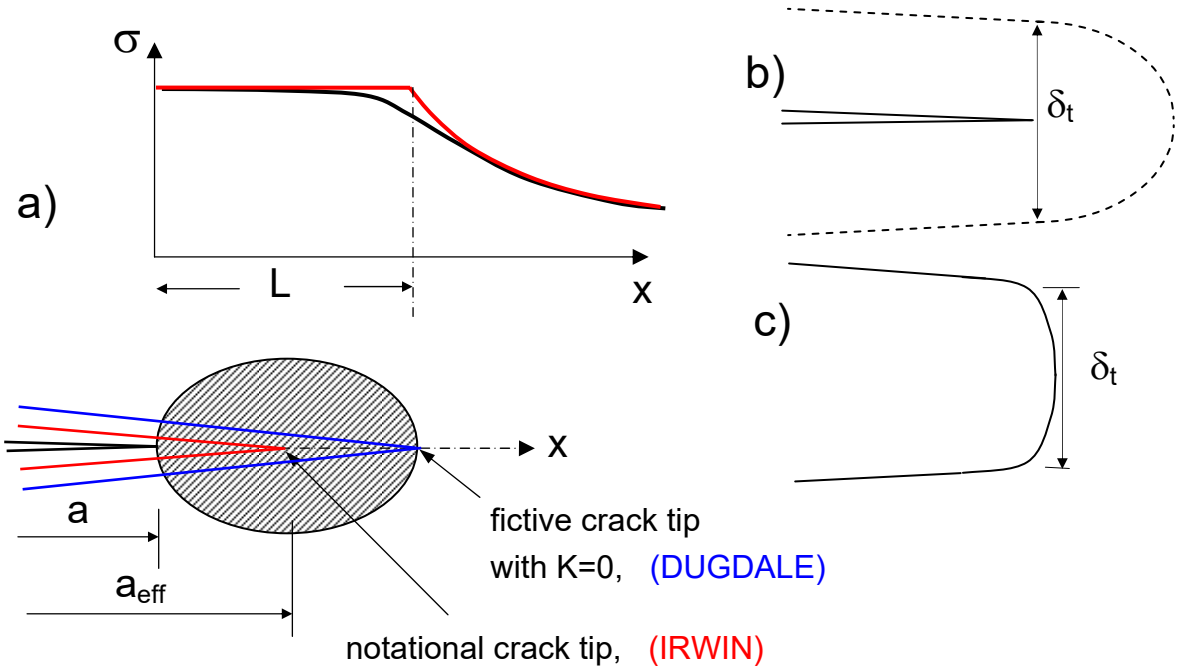

Fig. 3 a) Stress distribution curve near a crack tip (black curve) approximated by an elastic-"plastic" material behaviour (red curve) in the crack-tip region (zone shape is not necessarily a circle), b) crack tip opening displacement (CTOD) δ_t, c) observable crack profile.

5. Experimental observation

Since many years, the deformation behaviour at crack tips in silica is discussed controversially. On the one hand, the behavior is described purely elastic. On the other hand, plastic and viscous behavior is assumed. As an argument for the second interpretation the blunt crack opening behaviour measured by Bando et al. [9] on thin lamellas has

been given. In their paper the authors show COD-profiles of cracks under load which were produced in thin silica sheets of 20-40nm thickness. Two of the images by Bando et al. [9] show cracks which were damaged in air and rather rapidly transferred into the TEM-device. The squares of the COD are shown in Fig 4a (Fig. 1B and Fig. 2A).
A specimen was cracked with a needle and then soaked for 7 days in water of 90°C. The squares of COD are given by the black data points in Fig. 4a. The opening at the tip of the physical crack, called *Crack Tip Opening Displacement* (CTOD), δ_t, is in fracture mechanics defined somewhat arbitrarily as twice the COD in a distance of $r = ½\,\delta_t$ [10], ensuring the 90° angle, as is indicated in Fig. 4b.

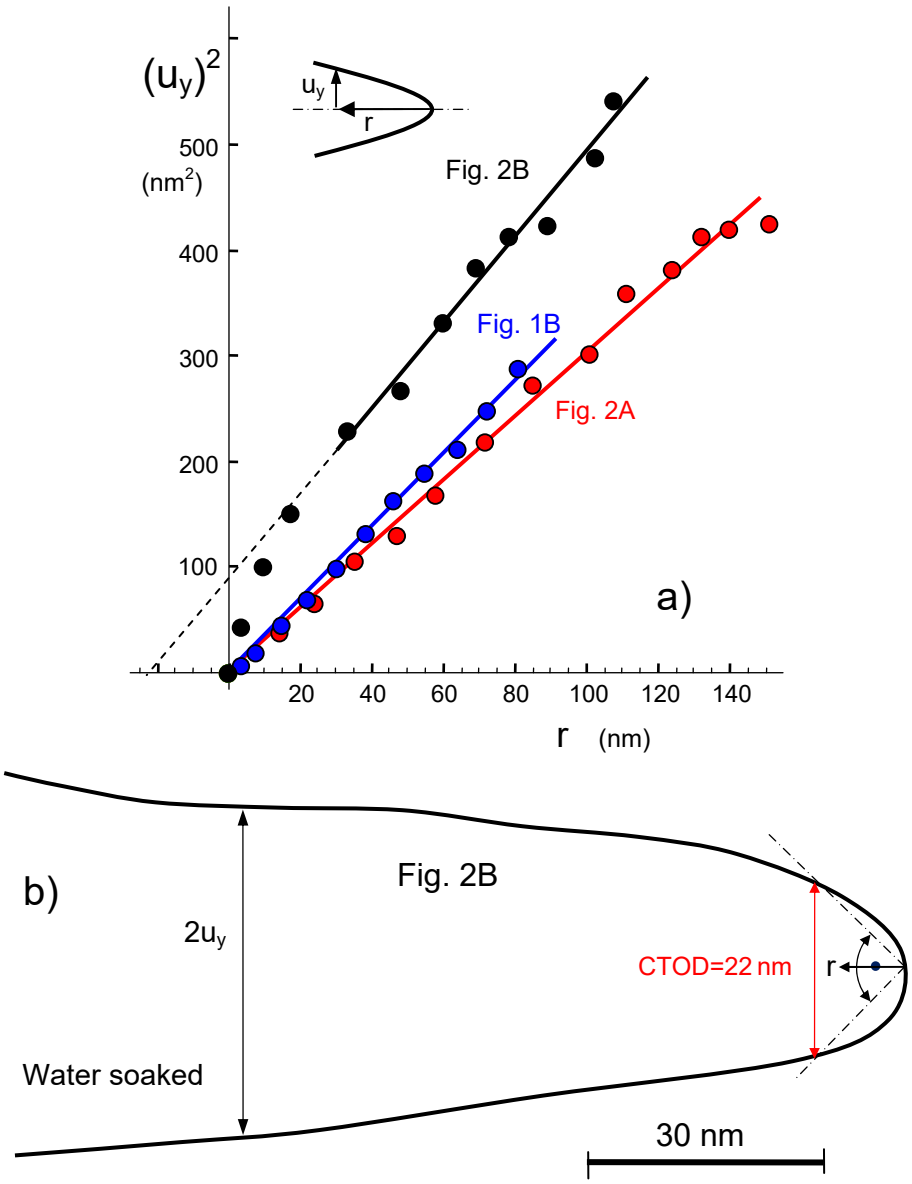

Fig. 4 a) Squares of crack opening displacements in dependence of the crack-tip distance, b) crack opening displacements for the water-soaked specimen, Fig. 2B of [9].

On the basis of this profile, Bando et al. [9] claimed that crack-tip blunting would occur at the tip. For an explanation of their blunting effect, they discussed a process of dissolution and precipitation, depending on the local curvature.
Very early this conclusion was questioned by Lawn et al. [11]. It was shown by these authors that an evaluation of crack opening displacements via the Irwin parabola results in an impossibly high stress intensity factor which was by a factor of 3-4 larger than the fracture toughness of K_{Ic}=0.8 MPa√m. Similar argumentation holds for the other cracks, too.
Lawn et al. [11] evaluated the COD of the crack in Fig. 2A (measured in humid air). They obtained over the distance of 150 nm from the crack tip:

$$K = 2.7 \pm 0.2 \text{ MPa}\sqrt{\text{m}} \tag{16}$$

In Fig.4a the squares of the displacements, $(u_y)^2$, are plotted versus the crack tip distance r for all cracks. Using the near-tip solution for the displacements (counted from the symmetry line to the crack surface), the so-called Irwin parabola,

$$u_y = \sqrt{\frac{8}{\pi}} \frac{K}{E} \sqrt{r} + O(r^{3/2}) \tag{17}$$

suggests linearity of the plots $(u_y)^2$=f(r) with the slope resulting in K. It should be mentioned that in fracture mechanics the displacements are the difference of the deformed structure to the undeformed one. From linear regression it results for the tests in air (90% CI in brackets)

$$K_{1B} = 2.65[2.62, 2.68] \text{MPa}\sqrt{\text{m}} \tag{18}$$

$$K_{2A} = 2.48[2.45, 2.51] \text{MPa}\sqrt{\text{m}} \tag{19}$$

and for the 7 days water-soaked crack

$$K_{2B} = 2.87[2.69, 3.04] \text{MPa}\sqrt{\text{m}} \tag{20}$$

The stress intensity factors obtained from the far-field displacements are all in good agreement with each other and agree with the result by Lawn et al. [11].
Results for zone length and CTOD were obtained by using the molar volume of $\Delta\overline{V} = 7.5\,\text{cm}^3/\text{mol}$ [12] and K_{appl} = 2.87 MPa√m. Depending on the model, the zone lengths L are about $L \approx 75$ nm and the crack tip opening displacements at about $\delta_t \approx 20$ nm as compiled in Table 1. The CTOD are in good agreement with the evaluation of the crack surface observations yielding ≈22 nm. The computations were performed with $E = E_0$ =72000 MPa.
The CODs in the near-tip region of Fig. 4b are somewhat blurred. There are several contours visible in the original image (Fig. 2B in [9]), shown in Fig. 5. We believe that

the thick contour represents the physical crack. The dashed curve shows a zone that extends over a distance of about 55 nm. A further shadowy recognizable contour is introduced in Fig. 5 by the dotted line. Under the assumption that this line might show the damaged zone, a zone length of L>75nm would result. This result agrees with the zone lengths for $\Delta\overline{V}$ =7.5 cm^3/mol. This is also the case for the CTOD results. The zone lengths of Table 1 are introduced in Fig. 5 as the shaded regions ahead the crack tip (red: Irwin, blue: Dugdale).

Model	$\sigma_{h,D,max}$	σ_Y	Zone length L	CTOD δ_t
Irwin	2109 MPa	6326 MPa	66 nm	23.0 nm
Dugdale	2109 MPa	6326 MPa	81 nm	18.1 nm

Table 1 Size L of the Irwin zone and of crack tip opening, δ_t, for the COD-profiles in Fig. 4. Applied stress intensity factor: K_{appl}=2.87 MPa$\sqrt{m}$. Computations carried out with E_0=72000 MPa and S_0=10^{-3} according to measurements by Zouine et al. (see [13] and [14]).

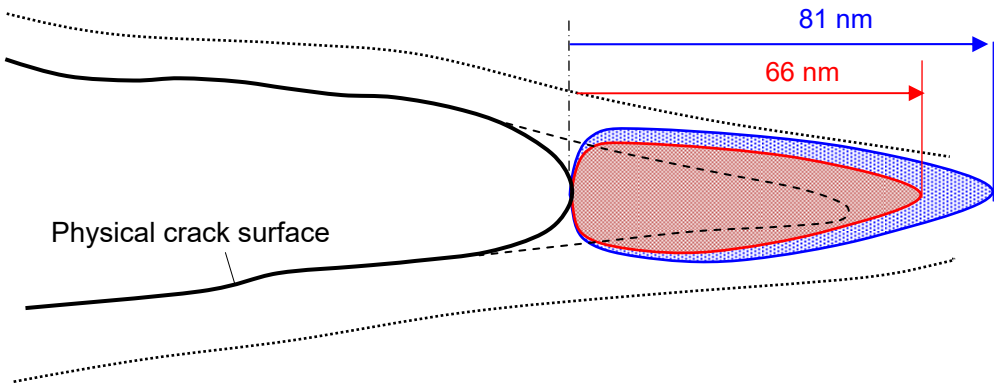

Fig. 5 Zone contours visible in the image 2B for the soaked specimen by Bando et al. [9], computed crack-tip zones compared with experimental ones, blue: model by Dugdale, red: model by Irwin.

6 Discussion

We evaluated the crack-tip opening displacement of the water-soaked specimen and obtained CTOD = 22.0 nm. In addition, we computed the CTOD by using the Irwin and the Dugdale models. These evaluations yielded CTOD = 18.1 nm for the Dugdale model and CTOD = 23 nm for the Irwin model. These astonishing agreements between experiment and computations suggest applying the elastic-plastic models for hydroxyl-damaged silica although the material remains elastic. The reason for this procedure is the rather good description of the deformation behavior by the bi-linear relation eq.(11). A certain disadvantage of the elastic-plastic approach is the fact that the method does not provide an explanation for the high K-factors. In a purely elastic analysis [15] we

could show, why the high applied stress intensity factors occurred. From this point of view, the purely linear-elastic approach in [15] is advantageous.
The transfer of relations (12) and (14) to the problem of hydroxyl-damaged crack tip zones is only possible if it is ensured that the water diffusion zone is greater than or equal to L. In the absence of molecular water, no damage can occur. This requirement is fulfilled in the experiments according to Bando et al. [9].
The thin sheet, which was water-soaked for 7 days at 90°C must show a stationary water concentration distribution. The reason is that water can diffuse from the two side surfaces (Fig. 6) with a diffusion length of

$$b = \sqrt{Dt} \tag{21}$$

The diffusivity is according to Zouine et al. [13] $D = 3\times10^{-19}\text{m}^2/\text{s}$. With $t = 7$ days $= 6\times 10^5$s it results $b \approx 400$ nm. This is much more than the half sheet thickness of $B/2 = 10$-20 nm. Therefore, any diffusion effects can be ignored for this test. In this case, the stress-enhanced water diffusion in the singular stress field cannot result in a separate diffusion zone. Even in the absence of stress enhancement, the diffusion depth compared to the specimen thickness is noteworthy.

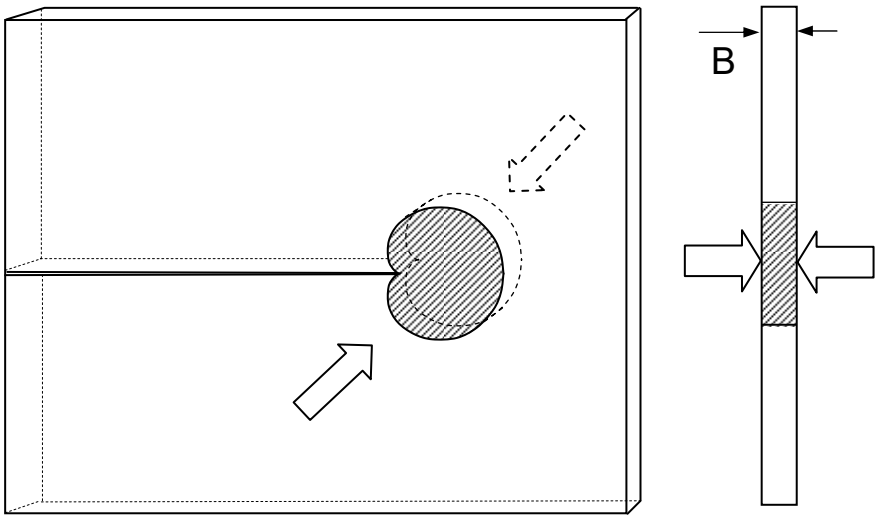

Fig. 6 Thin sheet of silica soaked with water from the side surfaces.

References

1 H. Le Chatelier, *C.R. Acad. Sci. Paris* **99**(1884), 786.

2 F. Lechenault, D.L. Rountree, F. Cousin, J.-P Bouchaud, L. Ponson and E. Bouchaud, "Evidence of Deep Water Penetration in Silica during Stress Corrosion Fracture," Phys. Rev. Let. **106**(2011), 165504.

3 T. Fett, G. Schell, C. Bucharsky, Hydroxyl Damage in Silica: Full-range description including large damages **126**, 2019, ISSN: 2194-1629, Karlsruhe, KIT.

4 K.K. Phani, S.K. Niyogi, A.K. De, Young's modulus of porous brittle solids, J. Mater. Sci. **22**(1987), 257–263.

5 D. Ashkin, R.A. Haber, J.B. Wachtman, Elastic properties of porous silica derived from colloidal gels, J. Am. Ceram. Soc., 73(1990), 3376-81.

6 *Mathematica*, Wolfram Research, Champaign, USA.

7 G. R. Irwin, Plastic zone near a crack and fracture toughness, Proc. 7th Sagamore Conf. 1960, p. IV-63 (1960).

8 D.S. Dugdale, "Yielding of steel sheets containing slits". J. Mech.Phys. Solids **8** (1960), 100-8.

9 Y. Bando, S. Ito, M. Tomozawa, Direct Observation of Crack Tip Geometry of SiO_2 Glass by High-Resolution Electron Microscopy, J. Am. Ceram. Soc., **67** (1984), C36 C37.

10 D.M. Tracey, Finite Element solutions for crack-tip behaviour in small-scale yielding, Trans. ASME, Ser. H, J. Engng. Materials and Technol. **98**(1976), 146-151.

11 B.R. Lawn, D.B. Marshall, A.H. Heuer, Comment on "Direct observation of crack tip geometry of SiO_2 glass by high-resolution electron microscopy", J. Am. Ceram. Soc. **67**(1984), C253.

12 T. Fett, K.G. Schell, S.M. Wiederhorn, Molar volume of SiOH estimated from swelling strains, Int. J. Appl. Glass Sci., **11**(2019), 608-611.

13 Zouine, A., Dersch, O., Walter, G., Rauch, F., Diffusivity and solubility of water in silica glass in the temperature range 23-200°C, Phys. Chem. Glasses, **48**(2007), 85-91.

14 T. Fett, G. Schell, Elimination of swelling stresses from measurements of the equilibrium constant in silica, **117**, 2019, ISSN: 2194-1629, Karlsruhe, KIT.

15 T. Fett, K.G. Schell, C. Bucharsky, G. Rizzi, Evaluation of crack profiles by Bando et al. - Application of COD-results from FE computations, **152**, 2021, ISSN: 2194-1629, Karlsruhe, KIT.

KIT Scientific Working Papers
ISSN 2194-1629

www.kit.edu